Hindawi
Advances in Materials Science and Engineering
Volume 2021, Article ID 4100896, 9 pages
https://doi.org/10.1155/2021/4100896

Research Article

Research on Intelligent Compaction Technology of Subgrade Based on Regression Analysis

Ziyi Hou,[1] Xiao Dang,[1] Yezhen Yuan,[2] Bo Tian,[3] and Sili Li[3]

[1]*School of Civil Engineering and Transportation, Hebei University of Technology, Tianjin 300401, China*
[2]*Chongqing Jiaotong University, Chongqing 400074, China*
[3]*Research Institute of Highway Ministry of Transport, Beijing 100088, China*

Correspondence should be addressed to Sili Li; decoli27@gmail.com

Received 7 June 2021; Revised 3 August 2021; Accepted 3 August 2021; Published 9 September 2021

Academic Editor: Yongsheng Yao

A remote monitoring system with the intelligent compaction index CMV as the core is designed and developed to address the shortcomings of traditional subgrade compaction quality evaluation methods. Based on the actual project, the correlation between the CMV and conventional compaction indexes of compaction degree K and dynamic resilient modulus E is investigated by applying the one-dimensional linear regression equation for three types of subgrade fillers, clayey gravel, pulverized gravel, and soil-rock mixed fill, and the scheme of fitting CMV to the mean value of conventional indexes is adopted, which is compared with the scheme of fitting CMV to the single point of conventional indexes in the existing specification. The test results show that the correlation between the CMV and conventional indexes of clayey gravel and pulverized gravel is much stronger than that of soil-rock mixed subgrades, and the correlation coefficient can be significantly improved by fitting CMV to the mean of conventional indexes compared with single-point fitting, which can be considered as a new method for intelligent rolling correlation verification.

1. Introduction

Subgrade soil settlement beneath pavements is a major concern for engineers [1]. Compaction plays an important role in improving the strength of the subgrade and pavement [2], and in long-term engineering practice, a variety of compaction quality evaluation indexes have been formed at home and abroad, mainly including two categories of physical testing indexes represented by compaction degree and mechanical indexes represented by elastic modulus [3, 4], although the testing methods and principles of these evaluation indexes are different, but most of them have low testing efficiency, poor representation, lagging results, and other disadvantages. With the continuous development of the engineering industry, there is an urgent need for a device that can test compaction with the vehicle, which can display the compaction test results in real time and guide the operator to operate reasonably. The corresponding detection systems have been developed in Sweden, Germany, USA, Japan, and China, and various compaction control indicators based on the harmonic method have been proposed, such as CMV [5–7] in Sweden and CCV [8–10] in Japan. Intelligent compaction technology can continuously and comprehensively reflect the compaction information of the subgrade, and when using the intelligent compaction system to quantitatively evaluate the compaction quality, the correlation between CMV and conventional indicators needs to be established, but this relationship is not fixed because CMV indicators are affected by multiple factors such as roller type, vibration frequency, and soil type. It is stipulated in JT/T 1127-2017 [11] that, before carrying out intelligent compaction control, the one-dimensional linear regression equation between the intelligent compaction index and the conventional index is established by point-to-point coordinate correspondence, and the correlation coefficient must be ensured to be above 0.7.

The existing intelligent compaction equipment is mainly oriented to the use of compaction operators, and the

secondary development is difficult and expensive to meet the requirements of actual projects. In view of this, this paper designs a subgrade intelligent compaction system with CMV as the core, using GPS technology [12], sensor technology [13], wireless transmission [14], and other key technologies to realize the real-time remote monitoring of compaction quality information.

Because the conventional fitting method does not consider the influence of the two testing methods in the roller wheel width direction on the correlation coefficient, this paper proposes an improved scheme for fitting CMV with the average value of conventional indicators along the wheel width direction, and relying on the Nanning Shajing-Wuxu Expressway project, three filler types of subgrades are selected to fit the relationship between CMV and conventional quality control indexes of compaction K and dynamic resilient modulus E [15–17], respectively.

2. Intelligent Laminating System

2.1. System Architecture. In order to realize the comprehensive real-time control of highway subgrade compaction and meet the integrated management needs of the compactor operator, construction unit, establishment unit, and owner, the design and development of the subgrade intelligent compaction system is carried out with the thinking of Internet of Things [18] as the guide. The overall architecture of the system is shown in Figure 1, which mainly contains the data acquisition layer, compaction data transmission layer, and application layer at the local end of the roller, where the data acquisition layer mainly includes hardware such as piezoelectric vibration sensors, GNSS antennas, 4G/WiFi antennas, data processing units, and intelligent display terminals. In the process of roller rolling, the vibration signal and high-precision positioning coordinate data of the vibrating wheel are unified and summarized with the data processing unit, and after certain algorithms are solved, compaction trajectory, compaction number, compaction thickness, compaction degree, and other compaction quality parameters are formed. The intelligent display terminal will visualize these data and provide key information in the form of images, figures, sounds, etc., to guide the compactor operator to operate reasonably.

The data transmission layer is mainly for 4G signal remote transmission to achieve effective data upload and data sharing among rollers. In view of the weak 4G network in some areas, wireless AP bridging network is used to solve the data transmission problem, and data transmission and sharing are realized through the WiFi module of the vehicle system.

The application layer mainly includes application service, data service, cloud platform access, and key indicator warning. With the background of the raster map [19], computer graphics and numerical values are used to dynamically display roller operation information, and managers can log in to the website to query the real-time dynamics of the roller, historical playback, quality reports, and many other contents, which can effectively improve management efficiency and save management costs, while the early warning system on the cell phone can push the information of the warning unqualified area in real time to achieve early detection of problems and early treatment and improve the process of construction quality control management.

2.2. Core Metrics Algorithm. The basic principle of intelligent compaction is to view the roller as a loading system acting on the subgrade and to reflect the compaction degree of the subgrade by using the spectrum analysis of the dynamic corresponding signal between the vibrating wheel and the soil, so as to realize the compaction quality detection of the whole rolling surface. The intelligent compaction system reflects the compaction degree size by the distortion degree of the acceleration signal, and its key index is the CMV, which is calculated by first collecting the compaction signal into the acceleration signal collector and then using the fast Fourier transform (FFT) [20, 21] technique for spectrum analysis to obtain the amplitude of each frequency component under different force states and find the fundamental frequency signal amplitude and the first harmonic amplitude. The intelligent compaction CMV corresponding to the intelligent compaction system can be expressed by the following equation [22]:

$$\mathrm{CMV} = C\frac{A_1}{A_0}, \tag{1}$$

where A_1 is the first harmonic amplitude, A_0 is the fundamental frequency signal amplitude, and C is a fixed constant.

As the data processing unit for acceleration signal processing, it is not possible to calculate all signals but only selectively intercept one section for calculation and analysis, which requires the use of window functions [23] to achieve; the common window functions are the rectangular window, triangular window, Hanning window, etc. After a comprehensive comparison of the applicability of the window functions, the Hanning window [11] is selected for signal calculation, and its function is

$$f(t) = \begin{cases} \dfrac{1}{T}\left(\dfrac{1}{2} + \dfrac{1}{2}\cos\dfrac{\pi t}{T}\right), & 0 \le |t| \le T, \\ 0, & |t| \ge T. \end{cases} \tag{2}$$

For every 20 cm of roller travel, the intelligent rolling system performs a data calculation, and the CMV over the full width of the roller's vibrating wheel is considered to be the same value.

3. Regression Analysis Field Test Protocol

3.1. Overview of the Test Site. The new project of Nanning Shajing-Wuxu Expressway is 25.8 km long, divided into two sections, most areas are filled with clay gravel and powdery gravel, and a few areas are filled with earth rock mixture; the basic physical properties of the filler are shown in Table 1.

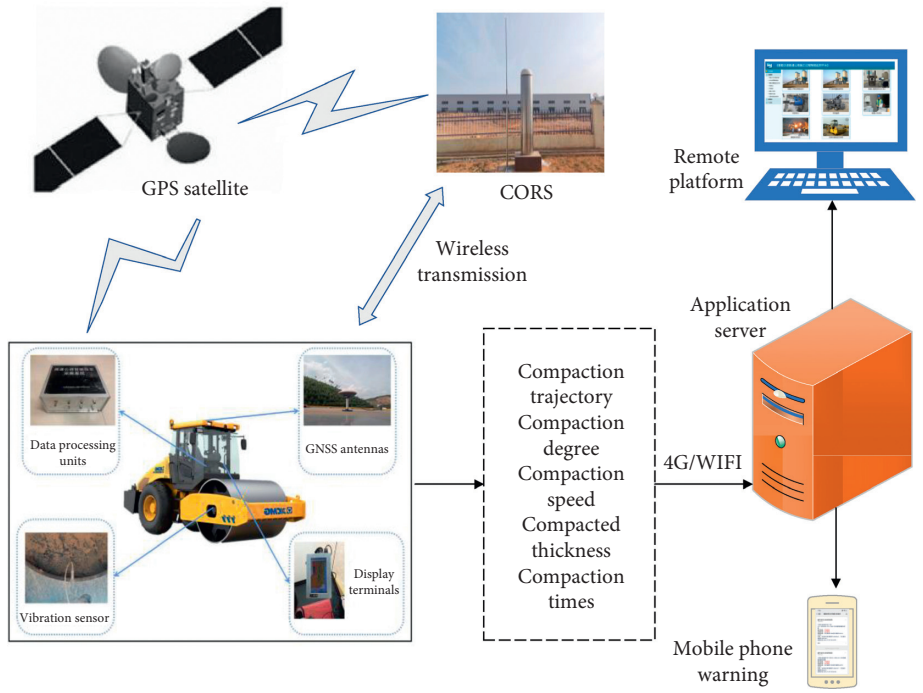

Figure 1: Overall system design diagram.

3.2. Test Equipment. This test involves the data collection of intelligent compaction index CMV and conventional compaction evaluation index, intelligent rolling equipment has been described in the previous section, conventional compaction index using compaction degree and dynamic resilient modulus, of which compaction degree is strictly in accordance with the "Highway Road Base Pavement Field Determination Procedure" JTG E60-2008 [24] requirements using the sand filling method of experimental determination, dynamic resilient modulus using KFD- 100A light falling hammer bending, and sinking instrument (PFWD); the basic parameters of the instrument are shown in Table 2.

Lightweight drop hammer-type bending instrument obtains load by impacting a rigid bearing plate located on the surface of the subgrade with the hammer falling freely, and the impact load and displacement due to the falling hammer are measured by load and acceleration sensors. The displacements are obtained by quadratic integration of the accelerations. In determining the modulus of resilient of the subgrade, the elastic half-space theory model was used for calculation [25, 26]. The dynamic resilient modulus is calculated as

$$E = \frac{\left(1 - v^2\right)p}{2rD}, \tag{3}$$

where E represents the dynamic resilient modulus measured by the system (MPa), P represents the load (N), D represents the displacement (m), r represents the radius of the bearing plate (m), and V represents Poisson's ratio.

Vibratory roller is the material carrier for the realization of intelligent rolling technology. To ensure the reliability of the data, XS263J, a roller model, is used for the whole experiment, and its basic performance parameters are shown in Table 3.

3.3. Test Methodology. The subgrade fill involved three forms of clayey gravel, pulverized gravel, and soil-rock mixed fill, so three test sections were selected to carry out the tests independently, and in order to ensure the comparability of the test results, the roller models, construction techniques, and test methods were identical at the three test sites.

In order to avoid the data collection being too concentrated and affecting the fitting effect, the roller was rolled 3 times and 5 times throughout 7 times along the three paths, and the system automatically generated the CMV of the rolling area during the rolling process. As shown in Figure 2, six inspection points were set up uniformly in each rolling area, and the spacing between adjacent inspection points in the same rolling strip was 10 m. In view of the lossy detection of sand filling, the dynamic resilient modulus E was firstly detected, and then the compaction was detected at the same position.

3.4. Fitting Method. Depending on the number of samples per test point and the fitting method, the correlation calibration can be further refined into the following two schemes.

3.4.1. Scheme 1: CMV and Conventional Index Single-Point Fit. From the perspective of GPS coordinate correspondence, the first scheme uses the point-to-point fitting

Table 1: Physical indicators of the filler.

Embankment type		Maximum dry density (g/cm^3)	Optimum moisture content (%)	Liquid limit (%)	Plastic limit (%)	Curvature factor	Unevenness factor
Earthwork Embankment	Clayey gravel	2.16	6.9	22.9	16.7	—	—
	Pulverized gravel	1.94	10.2	34.1	23.9	—	—
Soil and stone mixed fill		2.35	4.3	—	—	1.8	15.5

Table 2: PFWD performance parameters.

Projects	Performance parameters
Load-bearing plate diameter	100 mm
Falling height	50–530 mm
Load sensors	Rated range 20 kN
Acceleration sensor	Rated range 500 m/s^2
Height	1100 mm
Weight	15 kg

Table 3: Roller parameters.

Projects	Operating weight of the whole machine (kg)	Vibrating wheel width (mm)	Vibration frequency (Hz)	Nominal amplitude (mm)	Excitation force (kg)	Front wheel distribution mass (kg)	Rear wheel distribution mass (kg)	Vibrating wheel diameter (mm)
Parameters	26000	2170	27/32	1.9/0.95	405/290	13000	13000	1600

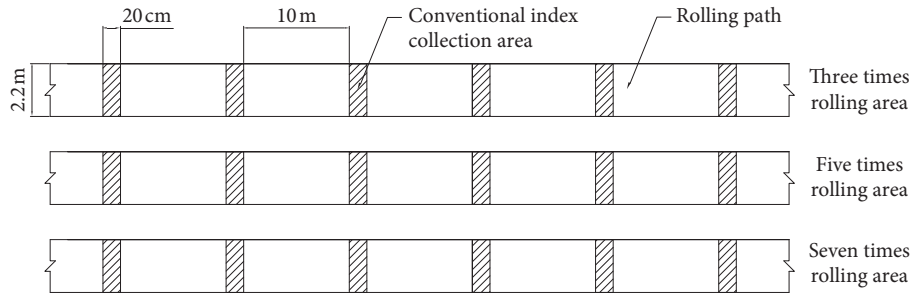

Figure 2: Overall arrangement of sampling points for conventional indicators.

method in JT/T 1127-2017. As shown in Figure 3(a), the compaction area represented by one CMV is a rectangular area of 2.2 m in length and 20 cm in width, and the conventional indexes are tested at the center of this area. In the end, one CMV, one dynamic resilient modulus, and one compaction value are collected at each test point, and a total of 18 test points are collected for the three compaction strips, generating 18 sets of such corresponding data for further fitting analysis.

3.4.2. Scheme 2: CMV and Conventional Index Mean Fit. The compaction value and dynamic resilient modulus reflect the compaction effect of a circular area with a diameter of about 20–30 cm, and the influence area is much smaller than the rectangular area represented by one CMV. Considering that the actual conventional indexes may have some variability along the wheel width direction, in order to reduce the influence of single-point abnormal data on the fitting effect, the test scheme was improved on the basis of scheme 1, and multiple points were carried out along the wheel width direction of the roller. The conventional indexes were collected as shown in Figure 3(b), and the average value of five detection points was used as the conventional indexes in the region and further linearly fitted with the CMVs.

3.5. Correlation Analysis of the CMV and Conventional Indicators

3.5.1. Establishing a Mathematical Model for the Calibration of Intelligent Compaction Indicators and Conventional Indicators. To establish the linear relationship between the CMV and conventional indicators, first, draw a scatter plot in a plane coordinate system with CMV as the x-coordinate and conventional indicators as the y-coordinate, and seek a straight line so that the sum of squares of the vertical

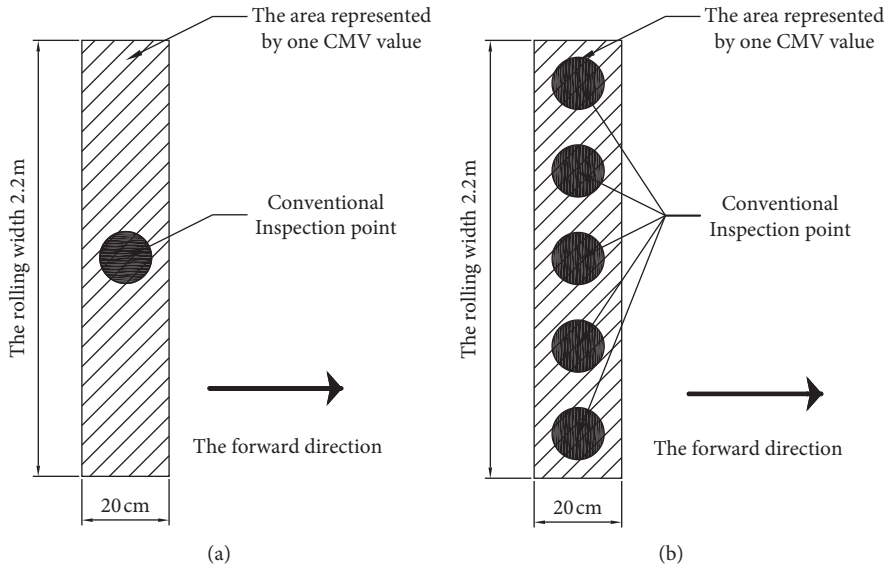

Figure 3: Fitting scheme. (a) Single-point fitting. (b) Multipoint mean fit.

distance from each scatter point to the line is minimized, that is, the minimum value point of the demand function:

$$S(a,b) = \sum_{k=1}^{m} \left[(a + bx_k) - y_k\right]^2. \tag{4}$$

Function (4) finds the first-order partial derivatives of the two variables a and b, respectively, giving

$$\begin{aligned} \frac{\partial S}{\partial a} &= 2\sum_{k=1}^{m}\left[(a + bx_k) - y_k\right], \\ \frac{\partial S}{\partial a} &= 2\sum_{k=1}^{m}\left[(a + bx_k) - y_k\right]x_k. \end{aligned} \tag{5}$$

Letting it to be equal to 0, the regular system of equations is obtained as

$$\begin{bmatrix} \mathrm{ma} + \sum_{k=1}^{m} bx_k = \sum_{k=1}^{m} y_k \\ \sum_{k=1}^{m} ax_k + \sum_{k=1}^{m} bx_k^2 = \sum_{k=1}^{m} x_k y_k \end{bmatrix}. \tag{6}$$

To determine the unknown parameters a and b in the regression equation, it is necessary to solve the regular system of equations:

$$\begin{bmatrix} m & \sum_{k=1}^{m} x_k & \cdots & \sum_{k=1}^{m} x_k^n \\ \sum_{k=1}^{m} x_k & \sum_{k=1}^{m} x_k^2 & \cdots & \sum_{k=1}^{m} x_k^n \\ \vdots & \vdots & \vdots & \vdots \\ \sum_{k=1}^{m} x_k^n & \sum_{k=1}^{m} x_k^{n+1} & \cdots & \sum_{k=1}^{m} x_k^{2n} \end{bmatrix} \begin{bmatrix} a_0 \\ a_1 \\ \vdots \\ a_n \end{bmatrix} = \begin{bmatrix} \sum_{k=1}^{m} y_k \\ \sum_{k=1}^{m} x_k y_k \\ \vdots \\ \sum_{k=1}^{m} x_k^n y_k \end{bmatrix}. \tag{7}$$

For each test in the field, the intelligent compaction value CMV and a single conventional compaction index (compaction or dynamic resilient modulus) comprised 18 sets of one-to-one corresponding two-dimensional data, and regression fitting was performed with the clayey gravel CMV and single-point compaction K. The collected test data are shown in Table 4.

A straight line fit of $y = a + bx$, with a and b being the regression coefficients, is performed on the data in Table 4, and substituting the data into the regular set of equations yields

$$\begin{bmatrix} 18 & 537.6 \\ 537.6 & 18107 \end{bmatrix} \begin{bmatrix} a \\ b \end{bmatrix} = \begin{bmatrix} 1656.5 \\ 50179.5 \end{bmatrix}. \tag{8}$$

The solution yields $a = 81.755$ and $b = 0.344$, so the fitted equation for the clayey gravel CMV and single-point compaction K is $y = 0.344x + 81.755$, i.e., $K = 0.344\mathrm{CMV} + 81.755$. To further verify the reliability of this regression equation fitting the actual data, a correlation test needs to be carried out, and the correlation coefficient is defined as

$$r = \frac{\sum_{k=1}^{m}(x_k - \overline{x})(y_k - \overline{y})}{\sqrt{\sum_{k=1}^{m}(x_k - \overline{x})^2 \sum_{i=1}^{n}(y_k - \overline{y})^2}}. \tag{9}$$

Substituting the data into equation (9), the correlation coefficient $r = 0.81$, and 0.7 is taken as the cutoff point for the strength of correlation in JT/T 1127-2017, which indicates that the clayey gravel CMV has a good correlation with the single-point compaction K and meets the needs of engineering applications.

3.6. CMV and Single-Point Conventional Index Fitting. Figure 4 shows the correlation verification results between the CMV and single-point compactness in the test section of clayey gravel, pulverized gravel, and soil-rock mixed fill. The

Table 4: Statistics of the CMV and single-point compaction of clayey gravel.

Serial number	CMV	Compaction degree K (%)	Serial number	CMV	Compaction degree K (%)
1	18.2	84.7	10	30	93.2
2	12.4	87.1	11	28.6	93.8
3	22.7	86.5	12	30.2	93.8
4	19.6	83.4	13	26	96.4
5	18.5	86.3	14	45.6	96.6
6	11.2	88.2	15	42.1	96.7
7	36.7	93.1	16	39.5	96.5
8	36.5	93.4	17	44.3	96.4
9	42.5	93.7	18	33	96.7

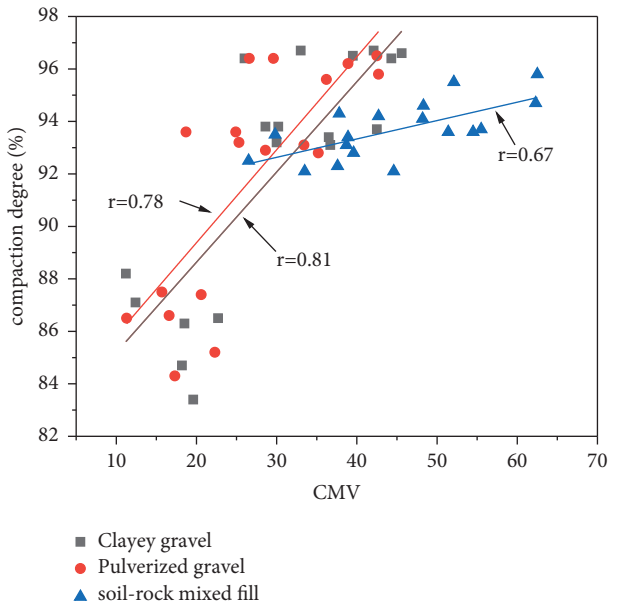

Figure 4: CMV and single-point compaction degree fit.

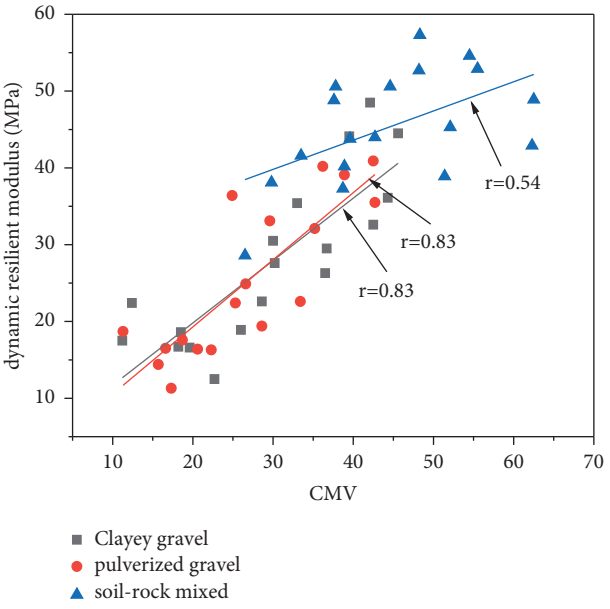

Figure 5: CMV and single-point dynamic resilient modulus fit.

correlation coefficients of the CMV and compaction in these three test sections are 0.81, 0.78, and 0.67, respectively. The correlation between the CMV and compaction is stronger for the clayey gravel and pulverized gravel sections, while the correlation between the CMV and compaction is weaker for the soil-rock mixed section. Figure 5 shows the correlation verification results between the CMV and single-point dynamic resilient modulus in the test section of clayey gravel, pulverized gravel, and soil-rock mixed fill. The correlation coefficients of the CMV and dynamic resilient modulus in these three test sections are 0.83, 0.83, and 0.54, respectively. Similarly, the correlation between the CMV and dynamic resilient modulus is stronger for the clayey gravel and pulverized gravel sections, while the correlation between the CMV and dynamic resilient modulus is weaker for the soil-rock mixed section.

3.7. CMV and Conventional Index Mean Fit. Figure 6 shows the correlation verification results between the CMV and compaction degree mean value, and the correlation coefficients for the clayey gravel, pulverized gravel, and soil-stone

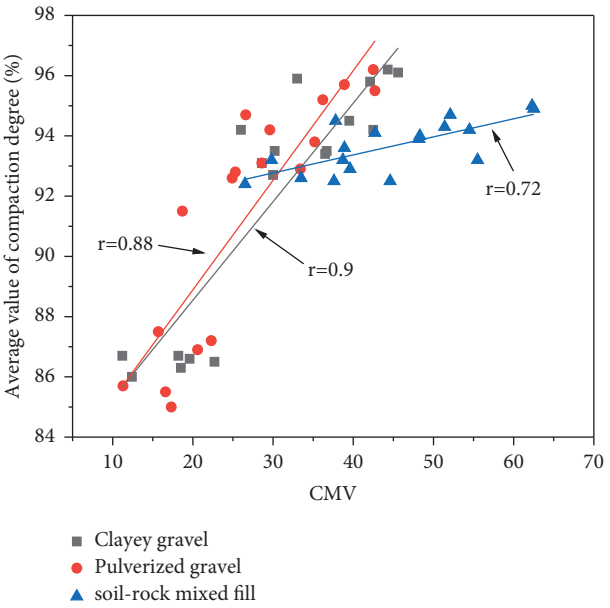

Figure 6: CMV and compaction degree mean value fit.

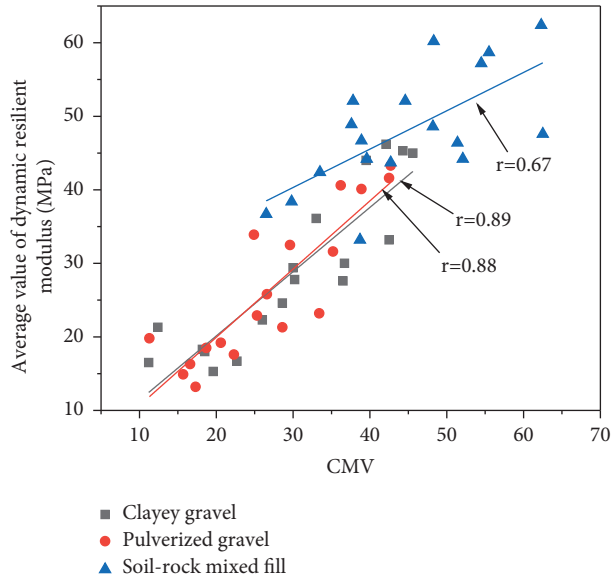

Figure 7: CMV and dynamic resilient modulus mean value fit.

Table 5: Correlations of different fitting schemes.

Fitting scheme	General indicators	Soil type	Regression equation	Correlation coefficient
Single-point fit of the CMV to conventional metrics	Compaction degree (%)	Clayey gravel	$Y = 0.34397x + 81.75453$	0.81
		Pulverized gravel	$Y = 0.35442x + 82.2894$	0.78
		Soil and stone mixed fill	$Y = 0.07004x + 90.53055$	0.67
	Dynamic resilient modulus (MPa)	Clayey gravel	$Y = 0.81216x + 3.57135$	0.83
		Pulverized gravel	$Y = 0.87405x + 1.81463$	0.83
		Soil and stone mixed fill	$Y = 0.38024x + 28.39997$	0.54
CMV and conventional index mean fit	Compaction degree (%)	Clayey gravel	$Y = 0.32728x + 81.99755$	0.9
		Pulverized gravel	$Y = 0.36386x + 81.61207$	0.88
		Soil and stone mixed fill	$Y = 0.05995x + 90.97041$	0.72
	Dynamic resilient modulus (MPa)	Clayey gravel	$Y = 0.87403x + 2.65116$	0.89
		Pulverized gravel	$Y = 0.9277 + 1.39252$	0.88
		Soil and stone mixed fill	$Y = 0.52152 + 24.67414$	0.67

mix sections are 0.9, 0.89, and 0.72, respectively. The correlation between the CMV and compaction degree mean value is relatively weak in the soil-stone mixed section, but it also meets the requirements of use. Figure 7 shows correlation verification results between the CMV and dynamic resilient modulus mean value, and the correlation coefficients for the clayey gravel, pulverized gravel, and soil-stone mix sections are 0.89, 0.88, and 0.67, respectively.

3.8. Comparative Analysis of the Fitting Effect. The correlation between the intelligent compaction index CMV and the conventional index compaction and dynamic resilient modulus under three kinds of subgrade fillers was established through field tests, and the correlation was checked for two fitting methods, point to point and point to average, and the correlation is shown in Table 5.

In order to further compare the differences between the two fitting methods, the correlation coefficients of point-to-point fitting and point-to-mean fitting were compared under different soils with the same conventional indexes, and the results are shown in Figure 8, which shows that the correlation coefficients of both the fitting of CMV and compaction and the fitting of the CMV and dynamic resilient modulus are higher than those of single-point fitting; especially, the mean fitting can improve the correlation coefficient of soil-rock mixed subgrade. The correlation coefficient between CMV and compaction can be improved from 0.67 to 0.72, from a weak correlation to a strong correlation, which is of great significance in practical applications. This indicates that

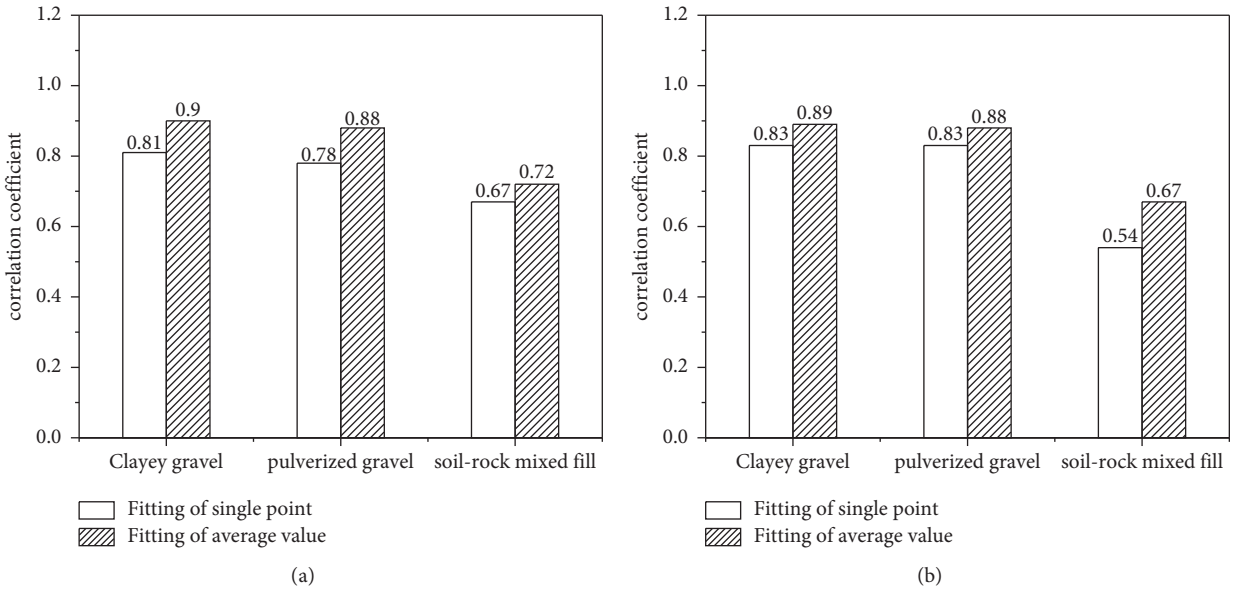

Figure 8: Comparison of correlation coefficients between single-point fit and mean fit. (a) Compaction fitting. (b) Dynamic resilient modulus fitting.

the improved fitting scheme can significantly improve the correlation between the CMV and conventional indexes.

4. Conclusion

(1) CMV of clayey gravel, pulverized gravel, and soil-rock mixed subgrade has a certain positive correlation with the conventional indexes (K and E), in which the correlation coefficients of clayey gravel and pulverized gravel are much higher than those of soil-rock mixed subgrade. It is recommended that the quality control of earth subgrade is carried out by the CMV, and the multi-indicator control method with CMV as the main and compaction number as the supplement is adopted for soil-rock mixed-fill subgrade to ensure the compaction quality meets the standard.

(2) Twelve linear regression equations determined by three filler types, two types of conventional indicators, and two fitting methods can be used as a reference for correlation calibration between the CMV and conventional indicators.

(3) The correlation between the CMV and single-point conventional indicators is weak, and the data are more volatile, while the correlation between the CMV and the mean value of conventional indicators along the wheel width direction is stronger, and the data fluctuate less, so the latter method is better to be fitted when analyzing the correlation between the CMV and conventional indicators.

Data Availability

The data used to support the findings of this study are included within the article.

Conflicts of Interest

The authors declare that they have no conflicts of interest.

References

[1] Y. Yao, J. Ni, and J. Li, "Stress-dependent water retention of granite residual soil and its implications for ground settlement," *Computers and Geotechnics*, vol. 129, Article ID 103835, 2021.

[2] G. Qian, K. Hu, J. Li, X. Bai, and N. Li, "Compaction process tracking for asphalt mixture using discrete element method," *Construction and Building Materials*, vol. 235, Article ID 117478, 2020.

[3] Z. Zhang, Z. Zhou, T. Guo et al., "A measuring method for layered compactness of loess subgrade based on hydraulic compaction," *Measurement Science and Technology*, vol. 32, no. 5, Article ID 055106, 2021.

[4] H. I. Park, G. C. Kweon, and S. R. Lee, "Prediction of resilient modulus of granular subgrade soils and subbase materials using artificial neural network," *Road Materials and Pavement Design*, vol. 10, no. 3, pp. 647–665, 2009.

[5] S. A. Kumar, R. Aldouri, S. Nazarian, and J. Si, "Accelerated assessment of quality of compacted geomaterials with intelligent compaction technology," *Construction and Building Materials*, vol. 113, pp. 824–834, 2016.

[6] C. L. Meehan, D. V. Cacciola, F. S. Tehrani, A. Jamshidi, and A. Doree, "Assessing soil compaction using continuous compaction control and location-specific in situ tests," *Automation in Construction*, vol. 73, pp. 31–44, 2017.

[7] N. W. Facas, R. V. Rinehart, and M. A. Mooney, "Development and evaluation of relative compaction specifications using roller-based measurements," *Geotechnical Testing Journal*, vol. 34, no. 6, pp. 634–642, 2011.

[8] S. Yoon, M. Hastak, and J. Lee, "Suitability of intelligent compaction for asphalt pavement quality control and quality assurance," *Journal of Construction Engineering and Management*, vol. 144, no. 4, Article ID 04018006, 2018.

[9] J. Ling, S. Lin, J. Qian, and J. Zhang, "Continuous compaction control technology for granite residual subgrade compaction," *Journal of Materials in Civil Engineering*, vol. 30, no. 12, Article ID 04018316, 2018.
[10] Q. Xu and G. K. Chang, "Evaluation of intelligent compaction for asphalt materials," *Automation in Construction*, vol. 30, pp. 104–112, 2013.
[11] Ministry of Transport China, "Technical Requirements for Continuous Compaction Control System of Fill Engineering of Subgrade for Highway," Ministry of Transport China, Beijing, China, JT/T 1127-2017, 2017.
[12] M. Castro, L. Iglesias, R. Rodríguez-Solano, and J. A. Sanchez, "Geometric modelling of highways using global positioning system (GPS) data and spline approximation," *Transportation Research Part C: Emerging Technologies*, vol. 14, no. 4, pp. 233–243, 2006.
[13] J. Hu, B. Zheng, C. Wang, C. H. Zhao, Q. Pan, and Z. Xu, "A survey on multi-sensor fusion based obstacle detection for intelligent ground vehicles in off-road environments," *Frontiers of Information Technology & Electronic Engineering*, vol. 21, pp. 675–692, 2020.
[14] O. E. Muogilim, K. K. Loo, and R. Comley, "Wireless mesh network security: a traffic engineering management approach," *Journal of Network and Computer Applications*, vol. 34, no. 2, pp. 478–491, 2011.
[15] A. Kavussi, K. Rafiei, and S. Yasrobi, "Evaluation of PFWD as potential quality control tool of pavement layers," *Journal of Civil Engineering and Management*, vol. 16, no. 1, pp. 123–129, 2010.
[16] V. George and A. Kumar, "Studies on modulus of resilience using cyclic tri-axial test and correlations to PFWD, DCP, and CBR," *International Journal of Pavement Engineering*, vol. 19, no. 11, pp. 976–985, 2018.
[17] J. Qian, Y. Yao, J. Li, H. Xiao, and S. Luo, "Resilient properties of soil-rock mixture materials: preliminary investigation of the effect of composition and structure," *Materials*, vol. 13, no. 7, p. 1658, 2020.
[18] R. Want, B. N. Schilit, and S. Jenson, "Enabling the internet of things," *Computer*, vol. 48, no. 1, pp. 28–35, 2015.
[19] B. Jenny, B. Šavrič, and J. Liem, "Real-time raster projection for web maps," *International Journal of Digital Earth*, vol. 9, no. 3, pp. 215–229, 2016.
[20] J. Hongxia, W. Hongfu, L. Jihong, and P. Ruru, "Development of image pattern for textile based on FFT," *International Journal of Clothing Science & Technology*, vol. 24, 2012.
[21] M. Garrido, "A new representation of FFT algorithms using triangular matrices," *IEEE Transactions on Circuits and Systems I: Regular Papers*, vol. 63, no. 10, pp. 1737–1745, 2016.
[22] W. Hu, X. Shu, B. Huang, and M. E. Woods, "An examination of compaction meter value for asphalt pavement compaction evaluation," *International Journal of Pavement Engineering*, vol. 19, no. 5, pp. 447–455, 2018.
[23] M. Das, R. Kumar, and B. Sahana, "Implementation of effective hybrid window function for ECG signal denoising," *Traitement du Signal*, vol. 37, no. 1, pp. 119–128, 2020.
[24] G. Wang, Z. Wang, and F. Meng, "Vertical vibrations of elastic foundation resting on saturated half-space," *Applied Mathematics and Mechanics*, vol. 28, no. 9, pp. 1199–1207, 2007.
[25] Ministry of Transport of the People's Republic of China, "Field test methods of subgrade and pavement for highway Engineering," MOT, Beijing, China, JTG E60-2008, 2008.
[26] A. N. Guz and T. V. Rudnitskii, "Contact interaction of an elastic punch and an elastic half-space with initial (residual) stresses," *International Applied Mechanics*, vol. 43, no. 12, p. 1325, 2007.